https://doi.org/10.5607/en23015
Exp Neurobiol. 2023 Aug;32(4):285-301.
pISSN 1226-2560 • eISSN 2093-8144

Original Article

Experimental Neurobiology

Gallic Acid Ameliorates Cognitive Impairment Caused by Sleep Deprivation through Antioxidant Effect

Xiaogang Pang[1,2†], Yifan Xu[3†], Shuoxin Xie[1], Tianshu Zhang[1], Lin Cong[1], Yuchen Qi[4], Lubing Liu[2], Qingjun Li[2], Mei Mo[2], Guimei Wang[2], Xiuwei Du[2], Hui Shen[1,5*] and Yuanyuan Li[1*]

[1]Innovative Institute of Chinese Medicine and Pharmacy, Shandong University of Traditional Chinese Medicine, Jinan 250355, [2]Experimental Center, Shandong University of Traditional Chinese Medicine, Jinan 250355, [3]Department of Medicine, Shandong University of Traditional Chinese Medicine, Jinan 250355, [4]School of Health, Shandong University of Traditional Chinese Medicine, Jinan 250355, [5]Department of Cellular Biology, School of Basic Medicine, Tianjin Medical University, Tianjin 300070, China

Sleep deprivation (SD) has a profound impact on the central nervous system, resulting in an array of mood disorders, including depression and anxiety. Despite this, the dynamic alterations in neuronal activity during sleep deprivation have not been extensively investigated. While some researchers propose that sleep deprivation diminishes neuronal activity, thereby leading to depression. Others argue that short-term sleep deprivation enhances neuronal activity and dendritic spine density, potentially yielding antidepressant effects. In this study, a two-photon microscope was utilized to examine the calcium transients of anterior cingulate cortex (ACC) neurons in awake SD mice in vivo at 24-hour intervals. It was observed that SD reduced the frequency and amplitude of Ca^{2+} transients while increasing the proportions of inactive neurons. Following the cessation of sleep deprivation, neuronal calcium transients demonstrated a gradual recovery. Moreover, whole-cell patch-clamp recordings revealed a significant decrease in the frequency of spontaneous excitatory post-synaptic current (sEPSC) after SD. The investigation also assessed several oxidative stress parameters, finding that sleep deprivation substantially elevated the level of malondialdehyde (MDA), while simultaneously decreasing the expression of Nuclear Factor erythroid 2-Related Factor 2 (Nrf2) and activities of Superoxide dismutase (SOD) in the ACC. Importantly, the administration of gallic acid (GA) notably mitigated the decline of calcium transients in ACC neurons. GA was also shown to alleviate oxidative stress in the brain and improve cognitive impairment caused by sleep deprivation. These findings indicate that the calcium transients of ACC neurons experience a continuous decline during sleep deprivation, a process that is reversible. GA may serve as a potential candidate agent for the prevention and treatment of cognitive impairment induced by sleep deprivation.

Key words: Sleep deprivation, Gallic acid, Oxidative stress, ACC

INTRODUCTION

Sleep deprivation (SD) is widely recognized as a contributing factor to various brain disorders, such as memory dysfunction and psychosis [1-3]. The influence of SD on cognition is significant, as adequate sleep time enables self-repair of nerve injury, removal of toxic metabolites produced by the body, and a reduction in cellular stress [4]. Both animal and human studies have demonstrated that sleep deprivation leads to memory impairment [5-7].

Cognitive impairments, including working memory and behavioral flexibility, have traditionally been linked to prefrontal cortex (PFC) dysfunction. Memory deficits due to sleep loss are observed in tasks that depend on the hippocampus, but also critically involve the medial PFC (mPFC) for consolidation. Sleep loss alters

Submitted April 20, 2023, Revised April 24, 2023,
Accepted April 30, 2023

*To whom correspondence should be addressed.
Yuanyuan Li, TEL: 86-0531-89628574, FAX: 86-0531-89628565
e-mail: lyy05_2012@163.com
Hui Shen, TEL: 86-0531-89628566, FAX: 86-0531-89626566
e-mail: shenhui@tmu.edu.cn
†These authors contributed equally to this article.

activation patterns in the PFC and its connections to the parietal cortex [8, 9]. Recent research has identified a PFC area in mice, the anterior cingulate cortex (ACC), which is functionally and anatomically positioned to control visually guided behaviors. Causal manipulation studies using chemical genetics or optogenetics have demonstrated the importance of ACC activity in visually guided tasks [10-12]. However, the exact role of ACC in cognitive impairment following SD remains to be elucidated.

Previous research has shown that SD promotes the accumulation of reactive oxygen species (ROS) [13], which can impair neural function and development leading to detrimental effects on cognitive functions, such as attention and working memory [14]. Neurons in the PFC are particularly susceptible to oxidative stress [15]. SD exacerbates oxidative stress in the PFC and reduces gamma activity, a prominent feature of the awake brain [16]. Therefore, it is hypothesized that oxidative stress induced by SD affects ACC neuronal activity, resulting in impaired cognitive memory.

Plant-derived natural products have been identified as effective molecules with neuroprotective activities for treating neurological diseases. Gallic Acid (GA, 3,4,5-trihydroxy benzoic acid), a low molecular weight phenolic compound, possesses antioxidant, anti-inflammatory, and neuroprotective properties [17, 18]. GA is readily absorbed and can cross the blood-brain barrier [19]. Furthermore, this molecule can be used to treat various neurological diseases that cause neuronal damage. GA has also been shown to prevent oxidative and neuronal damage by reducing glial activation, neuroinflammation, and protein aggregation [20]. However, it remains unknown whether the antioxidant GA can alleviate memory deficits caused by SD in mice.

In this study, continuous 72-hour sleep deprivation was combined with two-photon calcium imaging to observe cortical activity in the ACC layer II/III cortex in awake mice. Sleep deprivation was found to decrease the frequency and amplitude of Ca^{2+} transients and increase the proportions of inactive neurons. Furthermore, whole-cell patch-clamp recordings were employed in acute brain cortex slices to record glutamate receptor-mediated sEPSCs and gamma amino butyric acid A (GABAA) receptor-mediated spontaneous inhibitory postsynaptic currents (sIPSCs). These SD-induced neuronal and synaptic alterations suggest that ACC neurons may exhibit lower activity levels following sleep deprivation. In addition, the level of several oxidative stress parameters was assessed, and it was found that GA administration dramatically limited cortical inactivity and reversed the level of oxidative stress parameters. These findings suggest that GA exerts neuroprotective effects in sleep deprivation through the alleviation of oxidative stress.

MATERIALS AND METHODS

Animals

Male C57BL/6J mice (8 weeks old, 20~25 g) were obtained from the Institute of Zoology, Chinese Academy of Sciences. All mice had free access to food and water and were maintained in a temperature (22°C±2°C) and humidity (40%~60%) controlled room with a reverse light: dark cycle (12:12). Gallic acid powder (Sigma7384) was dissolved in saline (0.9%). Mice in the GA group received the same concentration (400 mg/kg) through gavage once a day at 5:30 p.m. Mice in the Control and SD groups were administered saline. Control: Saline. SD: SD+Saline. GA: SD+GA. All experiments were approved by the Animal Care and Use Committee of Shandong University of Traditional Chinese Medicine, in compliance with National Institutes of Health guidelines. Behavioral Assays.

Sleep deprivation procedure

The sleep deprivation procedure was performed based on a previously published method, with slight modifications [21, 22]. Mice were transferred to cylindrical sleep recording cages (25 cm in diameter and 40 cm tall, XINRUAN Technologies, China). During the sleep disruption period, the bar's rotation speed was set at 3 rotations per minute, with reversals of rotation direction (i.e., clockwise vs. counterclockwise) occurring at semi-random intervals of 10±10 seconds. The bar was programmed to rotate for 72 hours. Control animals were placed in identical cages with bars that remained stationary throughout the experiment. Cages were equipped with corncob bedding, and food/water was available ad libitum throughout the protocol.

Y-maze test

The Y-maze test was conducted according to a previously published protocol, with slight modifications [23]. Briefly, the Y-maze apparatus (XINRUAN Technologies, China) consists of three arms with identical dimensions (120°, 30 cm long×5 cm wide×15 cm high). The arms of the maze were labelled start, novel, and other. The camera was placed on the retort stand above the Y-maze and connected to a computer via an extended USB cable. The maze was placed inside a room with dim illumination (15~20 lux). The floor of the maze consists of sawdust to eliminate olfactory stimuli. Testing was always at the same time and performed in the same room to ensure environmental coincide. Place mice in behavioral testing room for 1 h before the test so they can acclimatize to the conditions.

After acclimatization of the mice, close off one of the arms labelled novel with the divider. Place the test animal into the start

https://doi.org/10.5607/en23015

arm, facing towards the center of the maze, holding the mice gently by the base of the tail. Let the mouse explore the maze undisturbed for 10 min. After the recording, return the test mouse to its home cage.

Clean all walls and the floor of the Y-maze before proceeding to the next animal. Wait 1 h and Remove divider. Place the same test mouse into the start arm, facing towards the center of the maze. Leave the animal to explore the maze undisturbed for 5 min. A mouse entry into an arm was considered valid if its body and tail completely entered the arm. The total number of arm entries and sequences were recorded using video and analyzed later on a computer. Remove mouse from the maze and place back into home cage. Spatial reference memory was assessed by identifying the start, novel, and other arms of the maze, recording the number of entries into each arm as well as the time spent in each arm [24].

Stereotaxic virus injection

Mice were anesthetized with an isoflurane-oxygen mixture (1.5% vol isoflurane/vol O_2) and administered the analgesic buprenorphine (SC, 0.3 mg/kg). Body temperature was maintained at 37±0.5°C with an electric heated pad during surgery. A 1 cm incision was made on scalp with an eye scissor. For calcium imaging with GCaMP6f, 150 nl of AAV2/1-syn-GCaMP6f-WPRE-hGH-containing solution (~2×10^{13} infectious units/ml) was slowly injected (50 nl/min) into the ACC (anterior/posterior: -0.27 mm, medial/lateral: +0.26 mm, and dorsal/ventral: -0.50 mm) using a glass microsyringe. The injection site refers to the previous research and has been slightly modified [25]. To prevent backflow during withdrawal, the pipette remained in the brain for over 15 minutes after completing the injection.

Implantation of custom-made head clamps

A round craniotomy (~4 mm diameter) in ACC of living mice was performed carefully and intermittently over the ACC. To improve imaging results, the skull and dura mater were carefully removed. A round glass coverslip (5 mm in diameter) was adhered over the opening with biological glue. Following surgery, animals were returned to their home cages and treated with carprofen (5 ug/g, bodyweight, i.p.) for a week.

Two-photon imaging in vivo

All imaging was performed using a two-photon microscope and a Ti: Sapphire laser (model "Mai-Tai Deep See" Spectra Physics). ZEISS water-immersion objectives (10X, 40X) were employed. For calcium imaging experiments, the excitation wavelength was set to 910 nm. The average power reaching the cortical surface ranged from 30 to 40 mW, depending on the expression efficiency of the virus and the depth of imaging. For somatic imaging, the field-of-view (FOV) dimensions were set to 200 μm×200 μm. Images of 512×512 pixels were acquired at a 4 Hz frame rate. Within an imaging time window of ~3 minutes (~1 minute per time, three times in total) for each imaging session, no signs of photodamage were observed. Imaging was performed at 6:30 p.m. each day. Prior to the experiment, mice were frequently fixed under the microscope objective with the chamber to acclimate to the imaging state for real calcium activity. When we observed neurons with a two-photon microscope for the first time, we first determined the approximate location of the ACC with a low magnification of the microscope (10X), and then decided the region of interest (ROI) based on the imaging quality and quantity of neurons in the field of vision with a high magnification of the microscope (40X). After the ROI was determined, the same ROI was observed each time by comparing the image characteristics of the blood vessels in the images as following steps. First, after the ROI was determined, the depth was determined (e.g. 350 um) and imaging was performed to determine the morphological characteristics of neurons or microvascular with a high magnification of the microscope (40X). Second, keeping X-axis and Y-axis unchanged, we changed the Z-axis to reduce the depth (eg. 50 um) and recorded the above features by imaging again. Third, we imaged ACC blood vessels with the low magnification of the microscope (10X) to record relative positions and characteristics of the vascular. On the next time of observation, after fixing the animal, we followed step third, second and first to find markers and the final ROI. In that way, the same ROI and the same neurons can be observed many times and multiple days.

Electrophysiology

The mice that were under deep anesthetization by breathed isoflurane were decapitated. The brains were rapidly dissected in precooled, oxygenated standard artificial cerebrospinal fluid (ACSF) (120 mM NaCl, 2.5 mM KCl, 2.4, 1.25 mM NaH_2PO_4, 26 mM $NaHCO_3$, 2 mM $MgSO_4$, 2 mM $CaCl_2$, 10 mM d-glucose; pH: 7.4). Both hemispheres were sliced coronally (350 μm) in cold ACSF. The slices were quickly transferred to 32°C ACSF for 30 min and then incubated at room temperature for at least 1 h. The slice was fixed in a recording chamber that was set on the fixed-stage of an upright Olympus BX50WI microscope (Olympus). The oxygenated ACSF was perfused through recording chamber continuously. Neurons in layer 2/3 were optically identified and whole-cell patched for recording.

Recording sEPSCs: brain slices were held between nylon netting in an interface chamber and fully submerged in flowing ACSF (3 ml/min) at room temperature (20~25°C). Cells in the ACC were

visualized using a DIC-infrared upright microscope and recorded using whole-cell patch-clamp procedures at -70 mV. The pipette resistance ranged from 4 to 6 MΩ. The intracellular solution contained (in mM): 140 K-gluconate, 2 $MgCl_2$, 10 HEPES, 10 BAPTA, 2 Mg-ATP, 0.5 $CaCl_2$-H_2O, 0.5 Li-GTP, pH 7.2~7.4, 280~290 mOsm. 5 mM QX-314 was added to block voltage-gated Na^+ channels and GABAB receptors. The sEPSCs were recorded in the presence of 100 μM picrotoxin (PTX).

Recording sIPSCs: Pipette electrodes were filled with an internal solution containing (in mM): 140 CsCl, 10 HEPES, 2 $MgCl_2$, 0.5 EGTA, 2 Mg-ATP, 0.5 Na_3GTP, 12 phosphocreatine, and 30 NMG, pH 7.2~7.4, 280~290 mOsm. To block voltage-gated Na^+ channels and $GABA_BRs$, 5 mM QX-314 was added. After voltage-clamping the neuron at -70 mV, sIPSCs were recorded in the presence of 1 mM kynurenic acid.

Recordings were conducted using a 2 kHz 4-pole Bessel filter at a 10 kHz sampling frequency with an Axopatch 700B amplifier and pClamp 10.3 software. Electrode capacitance and series resistance were monitored and compensated; access resistance was monitored throughout the experiment, and cells were discarded if access resistance increased more than 10% during the experiment.

Determination of antioxidant enzyme activities

Mice were anesthetized and euthanized, after which the cerebral cortex was quickly removed, homogenized, and centrifuged (12,000×g, 10 minutes, 4°C). Supernatants were collected for subsequent experiments. SOD activity and MDA level were measured using commercial assay kits (A003, A001, Nanjing Jiancheng Bioengineering Institute, Nanjing, China), with final results expressed as U/mg protein for SOD activity.

Nrf2 ELISA

Cortical tissues were rapidly dissected from the brain, flash-frozen in liquid nitrogen, and homogenized. The lysates were centrifuged at 1,000×g for 30 minutes. Supernatants were used to assess Nrf2 concentration. Nrf2 expression were quantified using ELISA kits (CSB-E16188m, CUSABIO, China) following the manufacturer's protocol.

Data analysis

Calcium imaging data preprocessing and cell segmentation were performed by using established methods [26-28]. Calcium imaging data were calibrated for motion artifacts and analyzed using custom-written software in MATLAB (version 2014a; MathWorks; MA). Movies focal plane displacements were corrected using Mosaic Package in MATLAB. After the ROI is determined, the same ROI is observed each time by comparing the image characteristics of the blood vessels in the images. To quantify calcium signal, somatic regions of interest (ROIs) fluorescence intensity were determined with a semi-automated algorithm that correlated the fluorescence intensity between adjacent pixels. The calcium signals of each ROI were averaged, and ROIs were confirmed again by visual inspection. Ca^{2+} signals were represented by relative fluorescence changes calculated as $\Delta f/f=(f-f0)/f0$, where f was estimated by averaging fluorescence of all pixels within each specified ROI, and f0 represented the baseline fluorescence of the ROI estimated as the 25th percentile of the fluorescence within a sliding time window. Cortical functional connectivity is defined as a strong temporal correspondence of events between two neurons [28]. Drastic motion imaging data were excluded from analyses. Electrophysiology data were filtered at 2 kHz and sampled at 10 kHz using an Axopatch 200B amplifier and pClamp 10.3 software. The amplitude and frequency of sEPSCs and sIPSCs were analyzed using MiniAnalysis (Synaptosoft, Inc). When possible, the Kolmogorov-Smirnov test was used. Otherwise, data points were assumed to have a normal distribution and were analyzed using a t-test or ANOVA followed by a post-hoc Tukey's test or Bonferroni's test. All data were two-sided and expressed as means±SEM. Statistical significance was considered at $p<0.05$.

RESULTS

Gallic acid ameliorates spatial learning and memory deficits in sleep-deprived mice

Sleep deprivation (SD) has been considered a contributing factor in various brain disorders, such as depression, memory dysfunction, and psychosis [29]. To evaluate the behavioral impact of SD regulation in mice, Y-maze behaviors were examined in mice subjected to a continuous 3-day sleep deprivation procedure and Gallic Acid (GA) exposure (400 mg/kg, once a day for 12 days; Fig. 1A). The 3-day sleep deprivation procedure resulted in a significant decrease in distance and time spent in the novel arm, which was reversed by GA exposure (Fig. 1B, 1C). No changes were observed in alternation ratio (Fig. 1D) and mean velocity (Fig. 1E) in both SD and GA-exposed mice. These findings suggest that GA treatment mitigates SD-induced spatial learning and memory deficits.

GA mitigated the decline in Ca^{2+} transients frequency and proportion of inactive neurons induced by SD

Previous research has demonstrated the significance of ACC activity in visually guided tasks [10-12]. To examine the changes in ACC cortical activity, the ultra-sensitive protein calcium sensor GCaMP6f was injected into the ACC (Fig. 2A~2C). A chronic

https://doi.org/10.5607/en23015

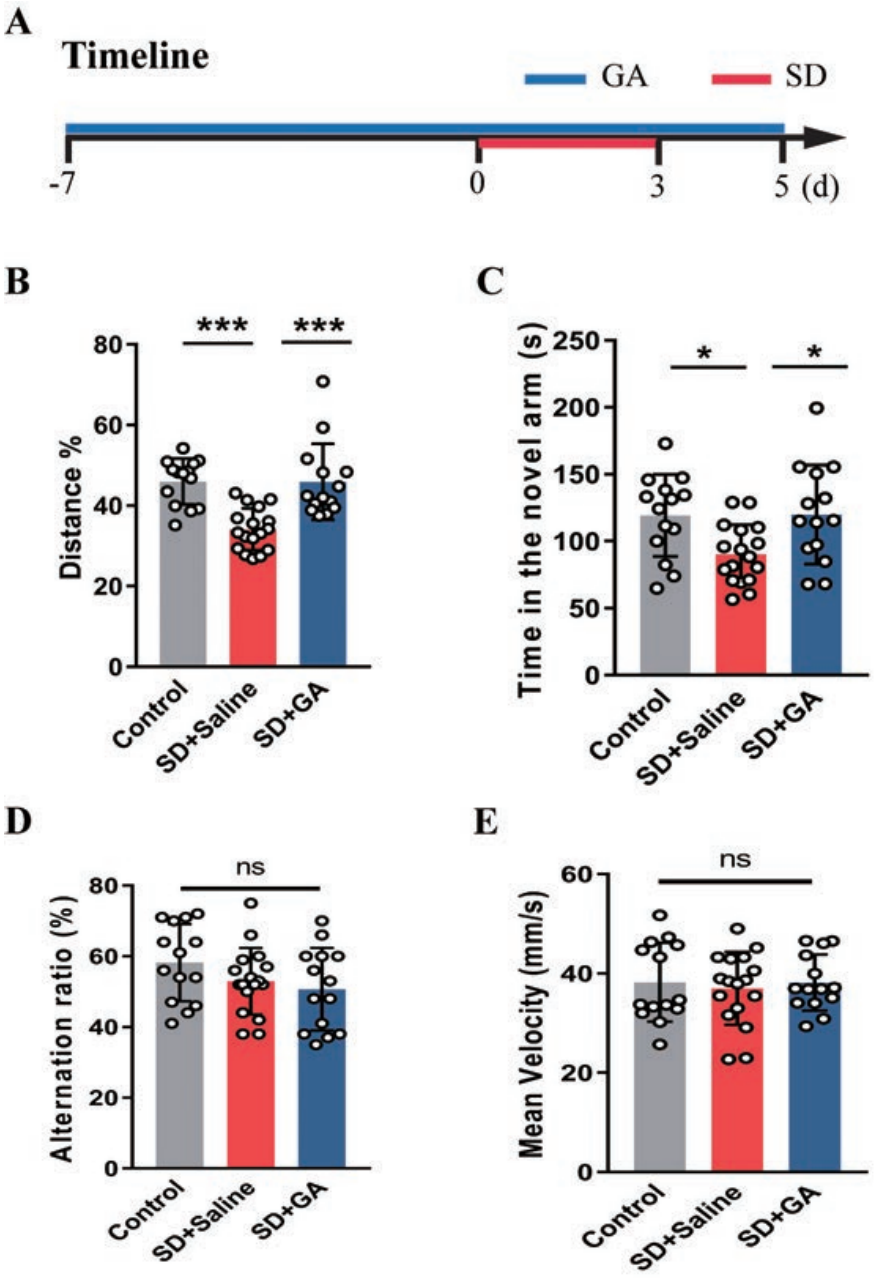

Fig. 1. Gallic acid (GA) improved spatial learning and memory deficits in sleep-deprived mice. (A) Time line of the experiment. Blue line, time period of GA; Red line indicates sleep deprivation for 72 h. (B) Percentage of distance in the Y-maze novel arm. Control vs. SD+Saline, p<0.001; SD+Saline vs. SD+GA, p<0.001. (C) Time in the Y-maze novel arm. Control vs. SD+Saline, p=0.032; SD+Saline vs. SD+GA, p=0.027. (D) Summary of spontaneous alternations in the Y-maze. Control vs. SD+Saline, p=0.529; SD vs. SD+GA, p>0.05. (E) The mean velocity in the Y-maze. Control vs. SD+Saline, p>0.05; SD+Saline vs. SD+GA, p>0.05. All data are shown as mean±SEM., *p<0.05, ***p<0.01, ns, not significant, one-way ANOVA with Tukey's test. Control mice, n=14; SD+Saline mice, n=17; SD+GA mice, n=14.

cranial window on the cortex was established to observe neuronal activity in layer II/III of the ACC in awake mice in vivo (Fig. 2D). Approximately three weeks later, two-photon calcium imaging was used to characterize the activity levels of neuron populations (350~450 μm) (Fig. 2E, 2F) with stably expressed GCaMP6f during the experiment.

To investigate the effects of SD and GA on neuron activity in the ACC, continuous sleep deprivation for 72 hours was performed in SD mice, and GA (400 mg/kg) was administered to GA mice for 12 days, starting seven days before SD. Representative calcium images of the same region of neurons at five time points during different periods of the experiment are shown (Fig. 3A; baseline,

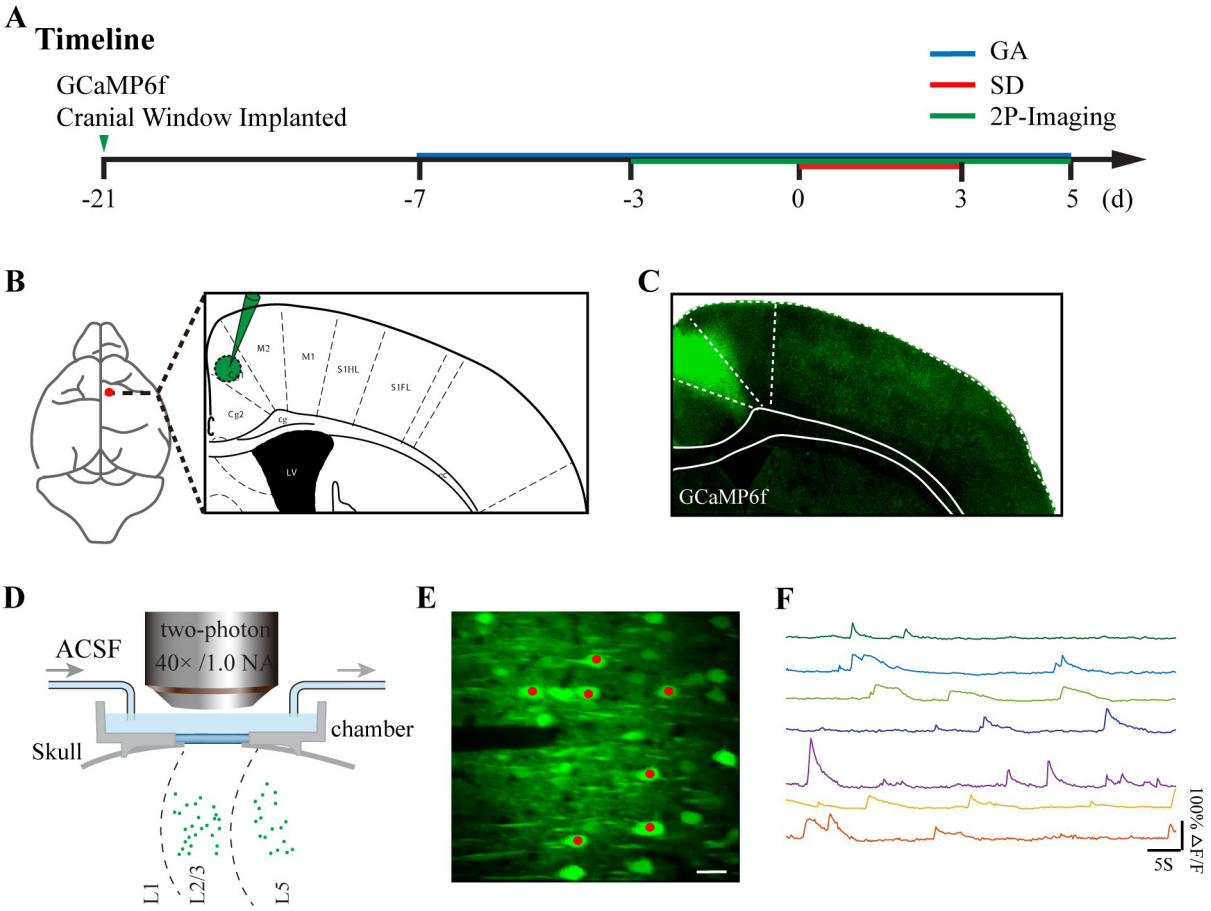

Fig. 2. GCaMP6f performance in the mouse anterior cingulate cortex (ACC). (A) Time line of the experiment. Green arrow, virus injection time; Blue line, time period of GA; Red line, sleep deprivation for 72 h; Green line indicates two-photon imaging time course. (B) Cartoon of virus injection sites. (C) Representative micrograph showing the site of GCaMP6f injection into ACC. (D) Schematic of two-photon imaging process. (E) Layer 2/3 cortical neurons imaged in vivo and activity maps. The neurons in the red dot are examples. (F) The spontaneous Ca^{2+} transients of neurons in (E) maps (scale bar, 10 um).

SD days 1~3, and recovery day 1). Neuron dysfunction was then observed to worsen. The average frequency of Ca^{2+} transients significantly decreased at 24, 48, and 72 hours of SD. A marked decrease was also observed on the first recovery day, but not the second day (Fig. 3B, 3D). Following GA exposure, the average frequency of Ca^{2+} transients significantly recovered, particularly at SD 72 hours (Fig. 3B, 3E, 3F). Based on the calcium transients, neurons were further classified into two categories: inactive cells (<3 Ca^{2+} transients/min) and normal cells (3~6 transients/min) to scrutinize the details of cortical activity in the ACC. The distribution of inactive cells in SD mice revealed a higher number of inactive neurons during SD. The proportion of inactive neurons increased on the first and second days of SD, but no significant differences were observed compared to the baseline (SD day 1: 33.3%, SD day 2: 38.1%, baseline: 18.5%) (Fig. 3G). However, continuous sleep deprivation for 72 hours led to a significant increase in the proportion of inactive neurons compared to the baseline (52.4% versus 18.5%). The changes in the proportion of inactive neurons were reversed by GA exposure (Fig. 3C, 3G). Collectively, these results demonstrate that GA effectively restricts the increase in the number of cortical inactive neurons and the decline in Ca^{2+} transients frequency induced by SD.

GA ameliorates the reduction in Ca^{2+} transients amplitude in ACC neurons

To characterize the changes in intracellular calcium concentration during SD and GA treatment, the mean amplitude of Ca^{2+} transients was analyzed. It was discovered that the mean amplitude of Ca^{2+} transients was significantly reduced at SD 24 hours (Fig. 4A, 4B). The mean amplitudes at SD 48 hours and SD 72 hours decreased, but no significant differences were observed compared to the baseline amplitude of Ca^{2+} transients (Fig. 4A, 4C, 4D).

https://doi.org/10.5607/en23015

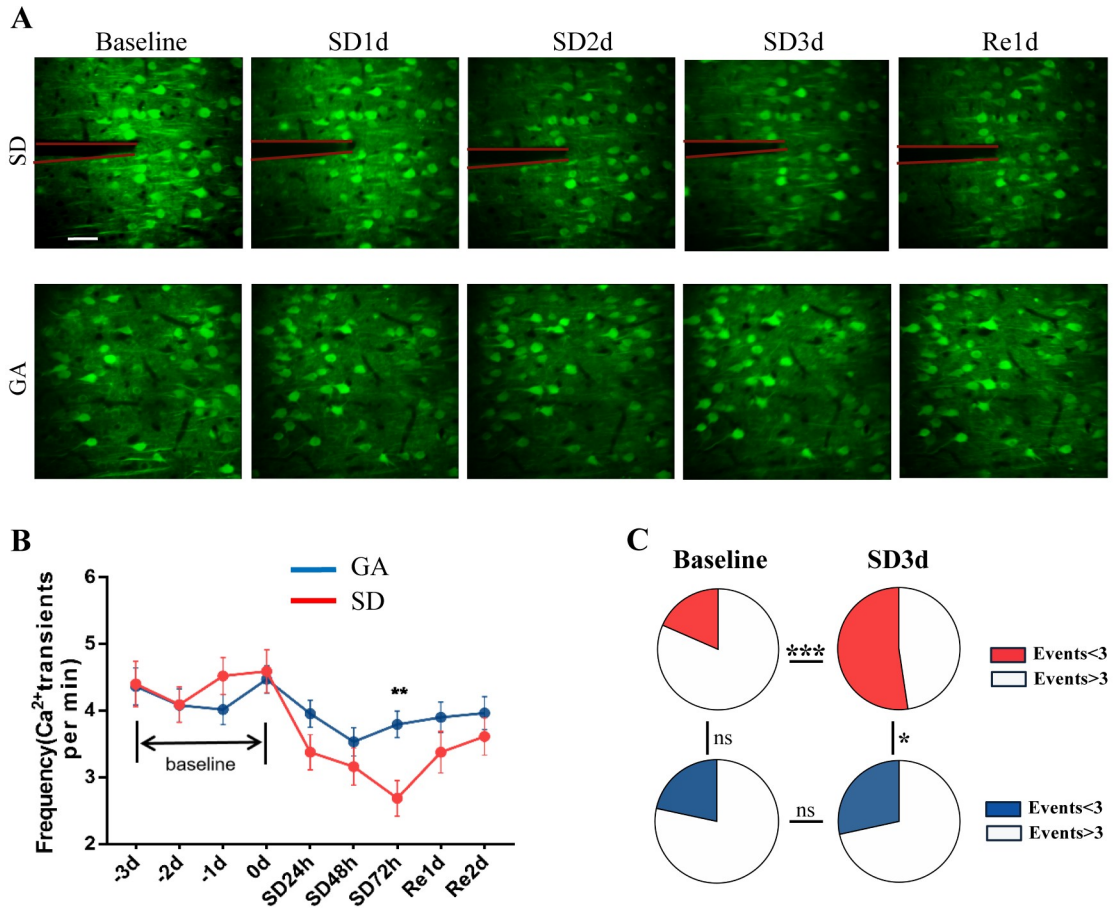

Fig. 3. GA limited the decrease of Ca^{2+} transients' frequency and the underactive neurons fractions at SD stage and remission stage in vivo. (A) Neurons in Layer II/III (300~450 um) of ACC imaged in vivo and activity maps in 0 days before, 3 days SD and one day after SD (from left to right) in SD (top) and GA mice (down), (Red line: The blood vessel, scale bar, 20 um). (B) The overall trend of the average frequency of Ca^{2+} transients during the whole experiment. Data are shown as mean±SEM., **p<0.01, Two-way ANOVA with Bonferroni's test. (C) The fractions of <3 Ca^{2+} transients/min in SD and GA mice. Two-tailed unpaired t-test. 0 d Baseline vs. 3 d SD+Saline, p<0.001; Baseline vs. GA-Baseline, p=0.543; 3 d SD: SD+Saline vs. SD+GA, p=0.012; GA+Baseline vs. 3 d SD+GA, p=0.360. (D) The average frequency of Ca^{2+} transients in SD 24 h, SD 48 h, SD 72 h, recover 1 d and recover 2 d compare with baseline time 0 d. Two-tailed paired t-test. 0 d Baseline vs. 24 h SD+Saline, p=0.024; 0 d Baseline vs. SD 48 h, p=0.004; 0 d vs. SD 72 h, p<0.001; 0 d vs. Re1d, p=0.019; 0 d vs. Re2d, p=0.082 (E) The average frequency of Ca^{2+} transients in 0 day, SD 24 h, SD 48 h, SD 72 h, recover 1 d in SD+Saline and SD+GA mice. Two-tailed unpaired t-test. 0 d: Baseline vs. GA+Baseline, p=0.747; SD 24 h: SD+Saline vs. SD+GA, p=0.104; SD 48 h: SD+Saline vs. SD+GA, p=0.315; SD 72 h: SD+Saline vs. SD+GA, p=0.002; recover 1 d: Saline vs. GA, p=0.194. n=42 cells in 6 SD+Saline mice, (F) The average frequency of Ca^{2+} transients in SD+GA group in SD 24 h, SD 48 h, SD 72 h, recover 1 d and recover 2 d compare with baseline time 0 d. Two-tailed paired t-test. 0 d Baseline vs. 24 h SD+GA, p=0.076; 0 d Baseline vs. 48 h SD+GA, p=0.002; 0 d Baseline vs. 72 h SD+GA, p=0.019; 0 d Baseline vs. Re1d SD+GA, p=0.066; 0 d Baseline vs. Re2d SD+GA, p=0.116, n=95 cells in 5 GA-treated mice. All data are shown as mean±SEM., ***p<0.001, **p<0.01, *p<0.05, ns, not significant. (G) The fractions of <3 Ca^{2+} transients/min in SD and GA mice. SD :SD+Saline. GA: SD+GA.

Additionally, a reflective enhancement but no difference in amplitude was observed after SD (Fig. 4N). However, GA treatment completely prevented the decrease in amplitude during SD and the enhancement of amplitude following SD (Fig. 4A, 4O). The amplitude in GA mice at SD 24 hours and SD 48 hours exhibited a significant increase compared to SD mice (Fig. 4F, 4G). No differences were observed at other time points between SD and GA mice (Fig. 4E, 4H, 4I, 4O). Subsequently, the rise time of Ca^{2+} transients was analyzed. No changes were detected during either SD or recovery time (Fig. 4J, 4L, 4O). Furthermore, both SD and GA exposure did not affect the fall time of Ca^{2+} transients (Fig. 4K, 4M, 4O). Collectively, these results suggest that GA exposure mitigates the decrease of Ca^{2+} transients amplitude induced by SD without altering the properties of Ca^{2+} transients.

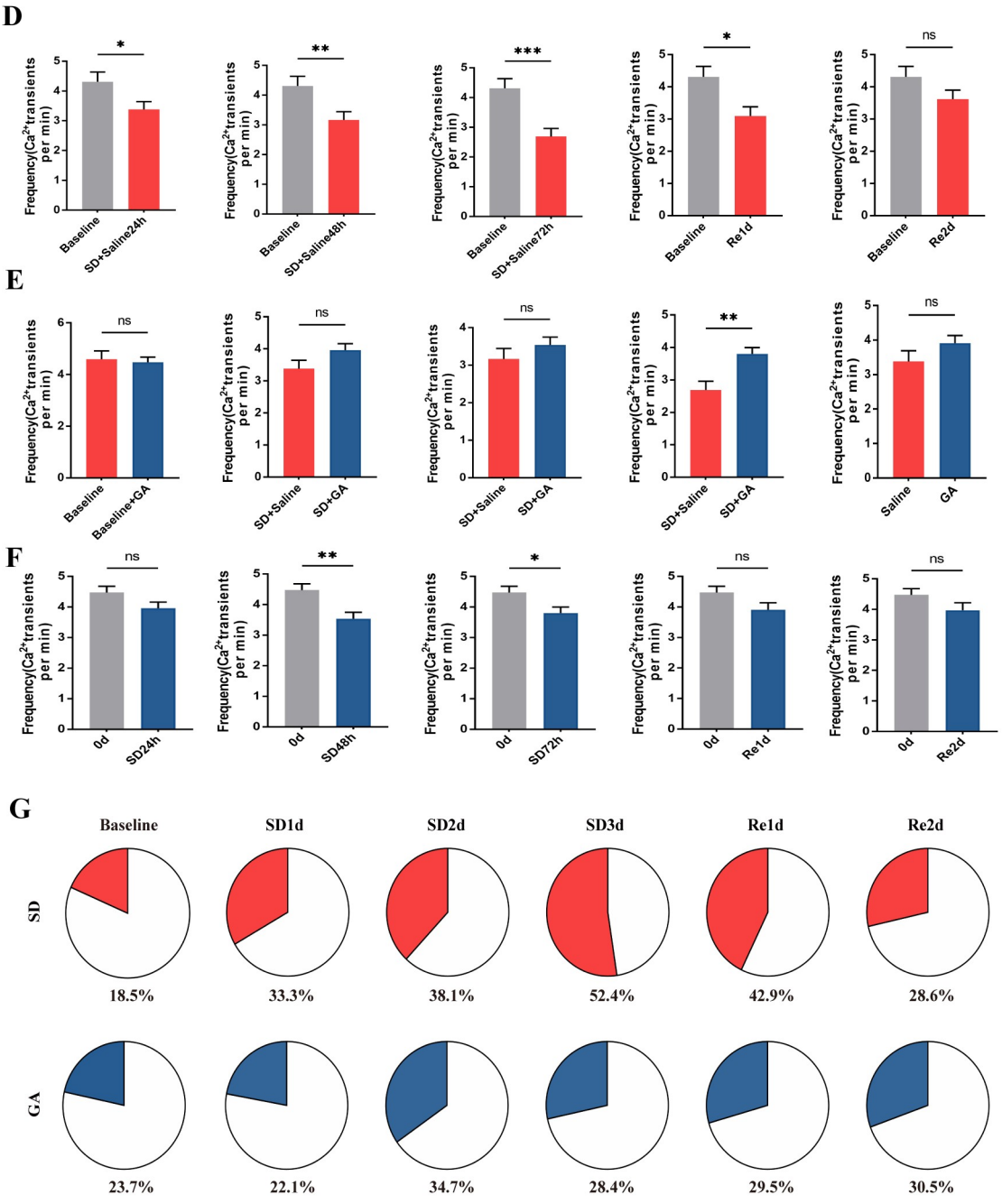

Fig. 3. Continued.

Continuous sleep deprivation for 72 hours and GA exposure do not affect the synchronization and functional connectivity of cortical network

Synchrony refers to the temporal consistency of distributed neuronal activity and serves as an indicator of information transfer capacity among neurons. High synchrony implies that more calcium events occur simultaneously. Functional connectivity is defined as a key measure of temporal correspondence of calcium transients between individual neurons. It represents the temporal causality of calcium events among neurons, which signifies functional communication. These two parameters were used to estimate temporal network activity patterns by calculating synchrony and correlation matrices quantifying network synchronization (Fig. 5A) and functional connectivity (Fig. 5B) among neurons in imaged regions, respectively. No significant differences were detected in network synchronization (Fig. 5C, 5E), suggesting no gross change in the

https://doi.org/10.5607/en23015

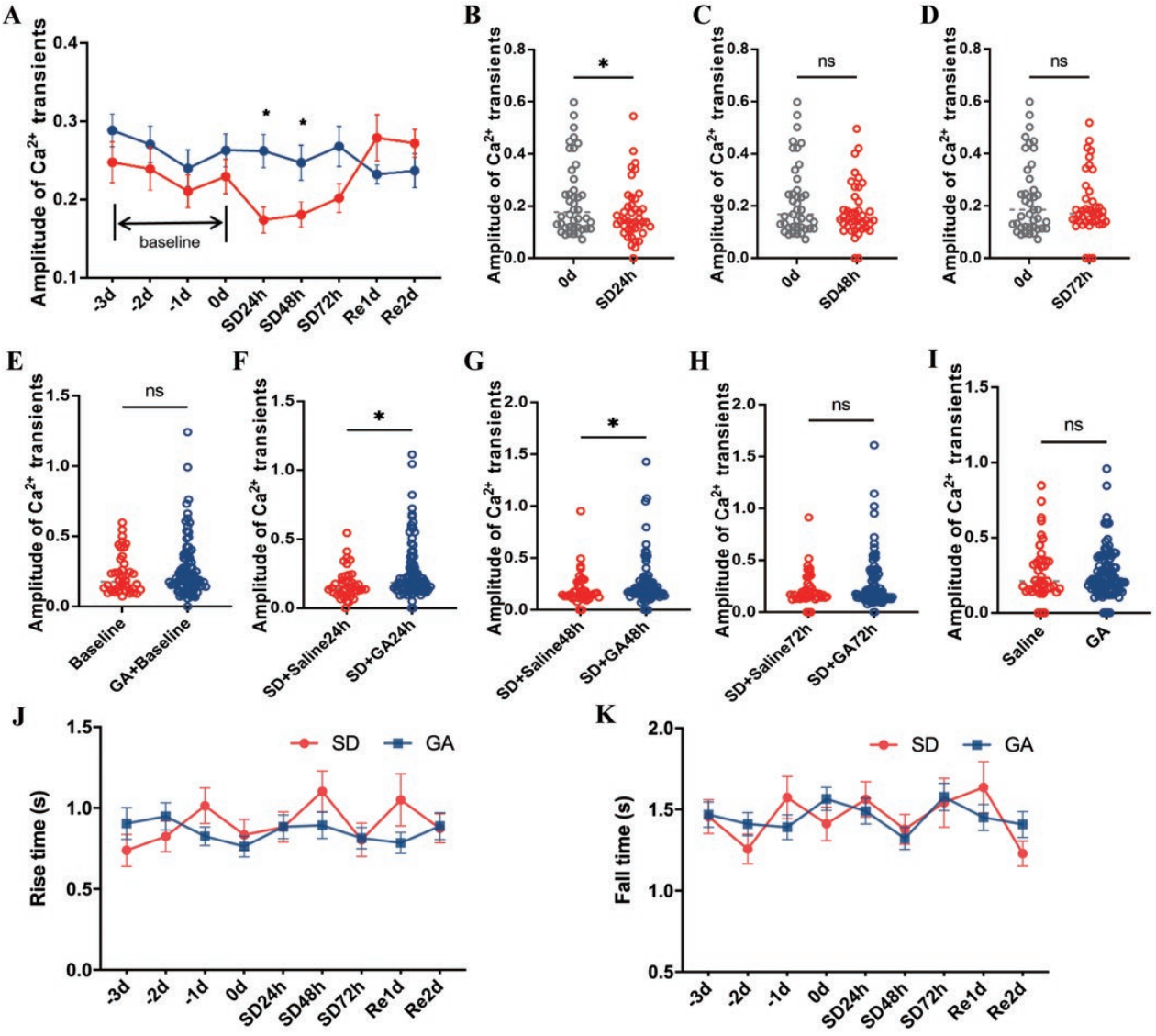

Fig. 4. GA modulated the change of calcium transient amplitude induced by SD. (A) Mean calcium transient amplitude of imaged regions daily after GA induction. SD 24 h: SD+Saline vs. SD+GA, p=0.038; SD 48 h: SD+Saline vs. SD+GA, p=0.02. (B~D) The mean amplitude of Ca^{2+} transients in SD 24 h, SD 48 h, SD 72 h compare with baseline time 0 d. Two-tailed paired t-test. 0 d Baseline vs. SD+Saline 24 h, p=0.039; 0 d Baseline vs. SD+Saline 48 h, p=0.336; 0 d Baseline vs. SD+Saline 72 h, p=0.740. (E~I) The mean amplitude of Ca^{2+} transients in 0 day, SD 24 h, SD 48 h, SD 72 h, recover 1 d in SD+Saline and SD+GA mice. Kolmogorov-Smirnov test. 0 d: Baseline vs. GA+Baseline, p=0.446; SD 24 h: SD+Saline vs. SD+GA, p=0.038; SD 48 h: SD+Saline vs. SD+GA, p=0.020; SD 72 h: SD+Saline vs. SD+GA, p=0.750; recover 1 d: Saline vs. GA, p=0.699 (J~K) The rise time (J) and fall time (K) of Ca^{2+} transients during the whole experiment. (L) The rise time of Ca^{2+} transients in SD 24 h, SD 48 h, SD 72 h in SD+Saline and SD+GA mice. Two-tailed unpaired t-test. SD 24 h: SD+Saline (40 cells) vs. SD+GA (91 cells), p=0.989; SD 48 h: SD+Saline (39 cells) vs. SD+GA (90 cells), p=0.168; SD 72 h: SD+Saline (39 cells) vs. SD+GA (88 cells), p=0.931. (M) The fall time of Ca^{2+} transients in SD 24 h, SD 48 h, SD 72 h in SD and GA mice. Two-tailed unpaired t-test. SD 24 h: SD+Saline (40 cells) vs. SD+GA (91 cells), p=0.609; SD 48 h: SD+Saline (39 cells) vs. GA (90 cells), p=0.634; SD 72 h: SD+Saline (40 cells) vs. SD+GA (88 cells), p=0.648. n=6 SD mice, n=5 GA-treated mice. All data are shown as mean±SEM., *p<0.05, ns, not significant. (N) The mean amplitude of Ca^{2+} transients in recover 1 d, recover 2 d compare with baseline time 0 d in the SD+Saline group. Re 1 d vs. 0 d in SD+Saline mice. p=0.071; Re 2 d vs. 0 d in SD mice. p=0.15. (O) The mean amplitude of Ca^{2+} transients in SD 24 h, SD 48 h, SD 72 h, recover 1 d, recover 2 d, compare with 0 d baseline in SD+GA mice. 24 h: 0 d Baseline vs. SD+GA, p=0.977; 48 h: 0 d Baseline vs. SD+GA, p=0.562; 72 h: 0 d Baseline vs. SD+GA, p=0.871; Re 1 d: 0 d Baseline vs. SD+GA, p=0.819; Re 2 d: 0 d Baseline vs. SD+GA, p=0.393. n=42 cells in 6 SD+Saline mice, n=95 cells in 5 SD+GA mice. All data are shown as mean±SEM., ns, not significant, Two-tailed paired t-test.

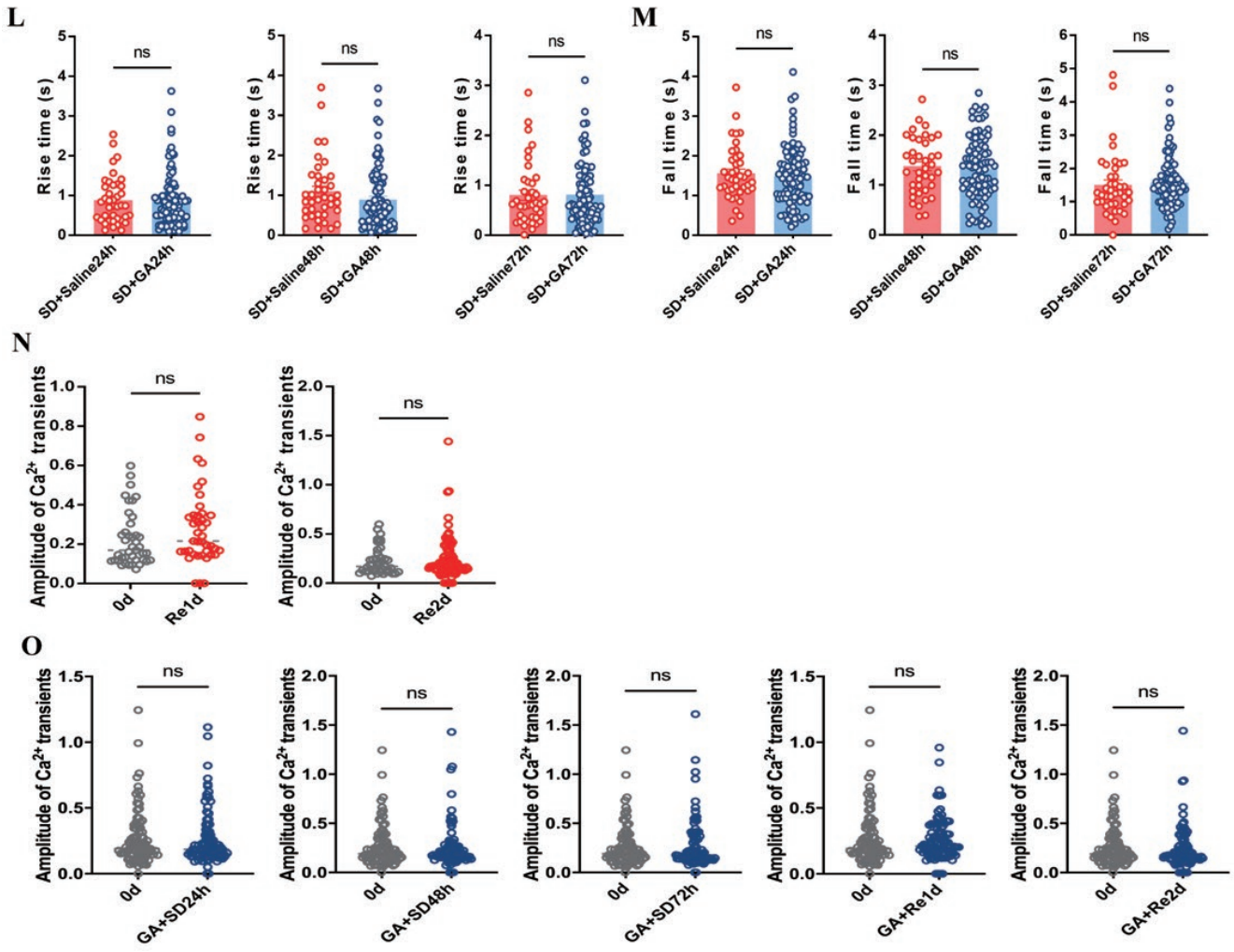

Fig. 4. Continued.

ability to transfer information among neurons during both SD and GA exposure. Subsequently, mean cell-cell correlation was assessed, and no changes were found in functional connectivity during SD and GA exposure (Fig. 5D, 5F). These results indicate that continuous sleep deprivation for 72 hours and GA exposure do not affect the synchronization and functional connectivity of the cortical network.

GA enhances frequency of glutamate receptor-mediated sEPSCs in SD

To investigate the functional consequences of changes in Ca^{2+} transients in neurons, whole-cell patch-clamp recordings were conducted on ACC neurons. Glutamate receptor-mediated spontaneous excitatory postsynaptic currents (sEPSCs) were measured (Fig. 6A), revealing that continuous sleep deprivation for 72 h and GA treatment did not affect the amplitude of sEPSCs (Fig. 6B). However, SD mice displayed a significant decrease in the frequency of sEPSCs, which was rescued by GA exposure (Fig. 6C). Neither the amplitude nor the frequency of GABAR-mediated spontaneous inhibitory postsynaptic currents (sIPSCs) were influenced by SD 72 h and GA exposure (Fig. 6D~6F). Data demonstrated a significant reduction in the frequency of sEPSCs following SD, but these changes were reversed to control levels after GA administration.

GA treatment may alleviate oxidative stress levels induced by SD

Several studies have indicated that SD triggers the accumulation of reactive oxygen species [13], which can impair neural function and development and have detrimental effects on cognition, including declines in attention and working memory [14], associated with alterations in the PFC [30]. The level of MDA, the activity of

https://doi.org/10.5607/en23015

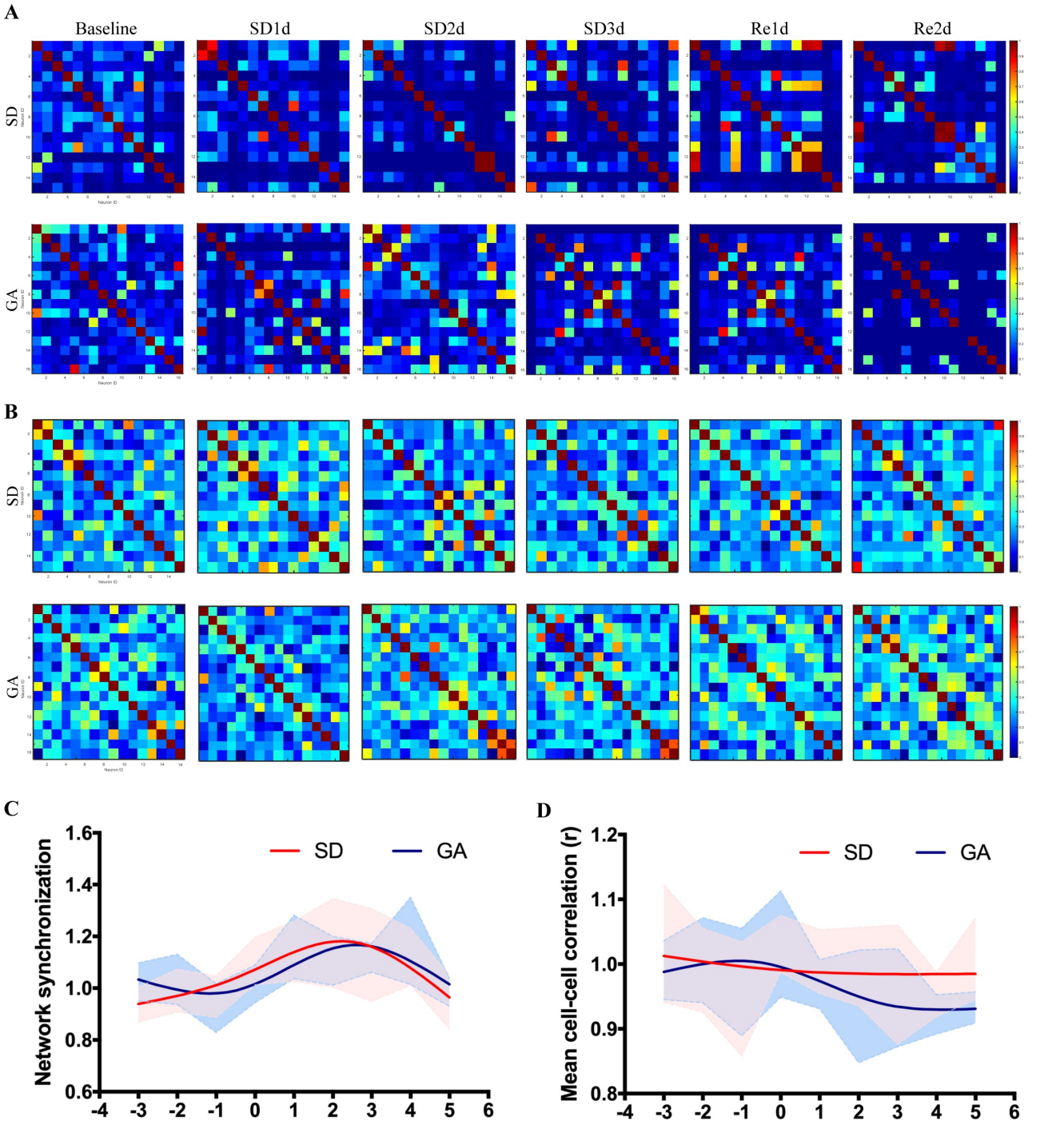

Fig. 5. The synchronization and functional connectivity of cortical network in SD and GA mice. (A) Raster plots depicting changes in activity (ΔF/F) over time for a representative correlation matrix quantifying network synchronization between each cell and every other. (B) Representative correlation matrices quantifying functional connectivity between each cell and every other spine. (C, D) The network synchronization and mean cell-cell correlation during the whole experiment. n=42 cells in 6 SD mice, n=95 cells in 5 GA-treated mice. All data are shown as mean±SEM. ns, not significant, two-way ANOVA with Bonferroni correction. SD: SD+Saline. GA: SD+GA. (E) The network synchronization in SD 24 h, p=0.923; SD 48 h, p=0.744 and SD 72 h, 0.958. n=6 mice in SD+Saline group, n=5 mice in SD+GA mice. (F) The functional connectivity of cortical network. SD 24 h, p=0.6; SD 48 h, p=0.569 and SD 72 h, p= 0.872. n=6 mice in SD+Saline group, n=5 mice in SD+GA group. All data are shown as mean±SEM. ns, not significant, two-tailed unpaired t-test.

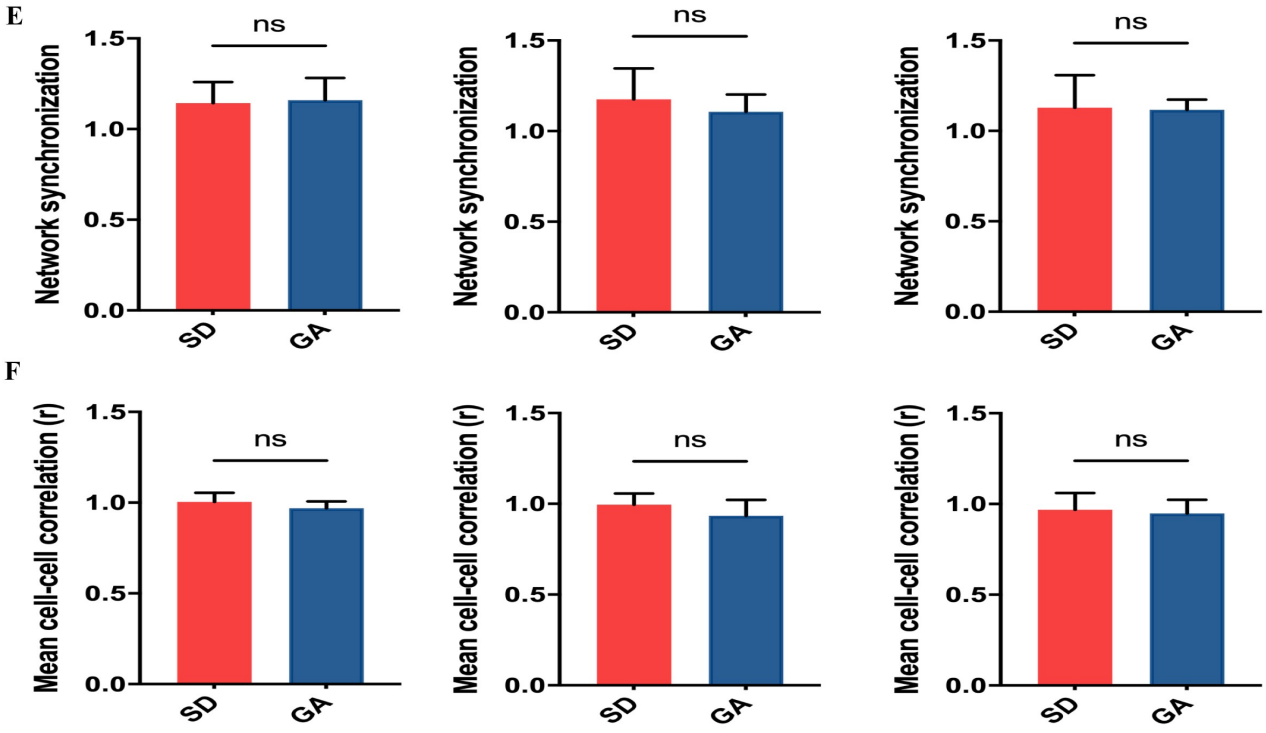

Fig. 5. Continued.

SOD, and expression of Nrf2 in different groups was subsequently examined. MDA levels were found to be significantly increased in SD mice compared to control mice, while GA administration notably decreased MDA levels (Fig. 6G). Additionally, it was discovered that SD weakened the activity of SOD and the expression Nrf2, while GA treatment counteracted the effects of SD. These results suggest that GA treatment can mitigate oxidative stress levels caused by SD.

DISCUSSION

The present study highlights the exacerbation of neuronal dysfunction in the ACC following continuous SD for 72 h, encompassing the average frequency and amplitude of Ca^{2+} transients and the proportion of inactive neurons (<3 Ca^{2+} transients/min). Furthermore, whole-cell patch-clamp recordings revealed a significant decrease in sEPSCs frequency, while the amplitude remained unchanged. These findings align with a report demonstrating a similar decrease in the excitability of PFC pyramidal cells following SD [31]. Additionally, the impact of SD on ACC neurons in layer II/III resembles the observations in subcortical neurons, such as rat hippocampal CA1 neurons, where SD induces considerable downregulation of excitability after 72 h of SD or 24 h of sleep fragmentation [23-34]. However, an increase in intrinsic excitability was observed in dorsal hippocampal CA1 neurons due to 24 h SD, alongside an increase in apical dendritic spines [35]. In layer V/VI pyramidal cells of the medial prefrontal cortex, intrinsic membrane excitability increased after 8 h of SD [36]. Despite differences in SD duration and methodology, these observations contrast with the current study's findings of decreased cortical excitability, indicating that various brain regions respond differently to sleep loss.

The significant decrease in the frequency of glutamate receptors observed suggests that the synaptic efficacy of ACC neurons declines following SD. This contrasts with a report where an increase in both the amplitude and frequency of mEPSCs was observed in neurons within layer II/III of the frontal association cortex from rats and mice after 4 h SD by gentle handling [37]. Miniature excitatory postsynaptic currents amplitude was slightly reduced, and miniature inhibitory postsynaptic currents amplitude remained unaffected in layer V/VI pyramidal cells of the medial prefrontal cortex [36]. These seemingly inconsistent results may reflect that SD differentially modulates distinct brain regions, rather than merely exerting global effects on the brain [38]. Additionally, it was shown that the concentration of extracellular glutamate increased during the first 3 h of sleep deprivation in rats [39], but decreased rapidly when sleep deprivation continued and high sleep pressure developed. In a 6 h SD, glutamate level decreased by approximately

https://doi.org/10.5607/en23015

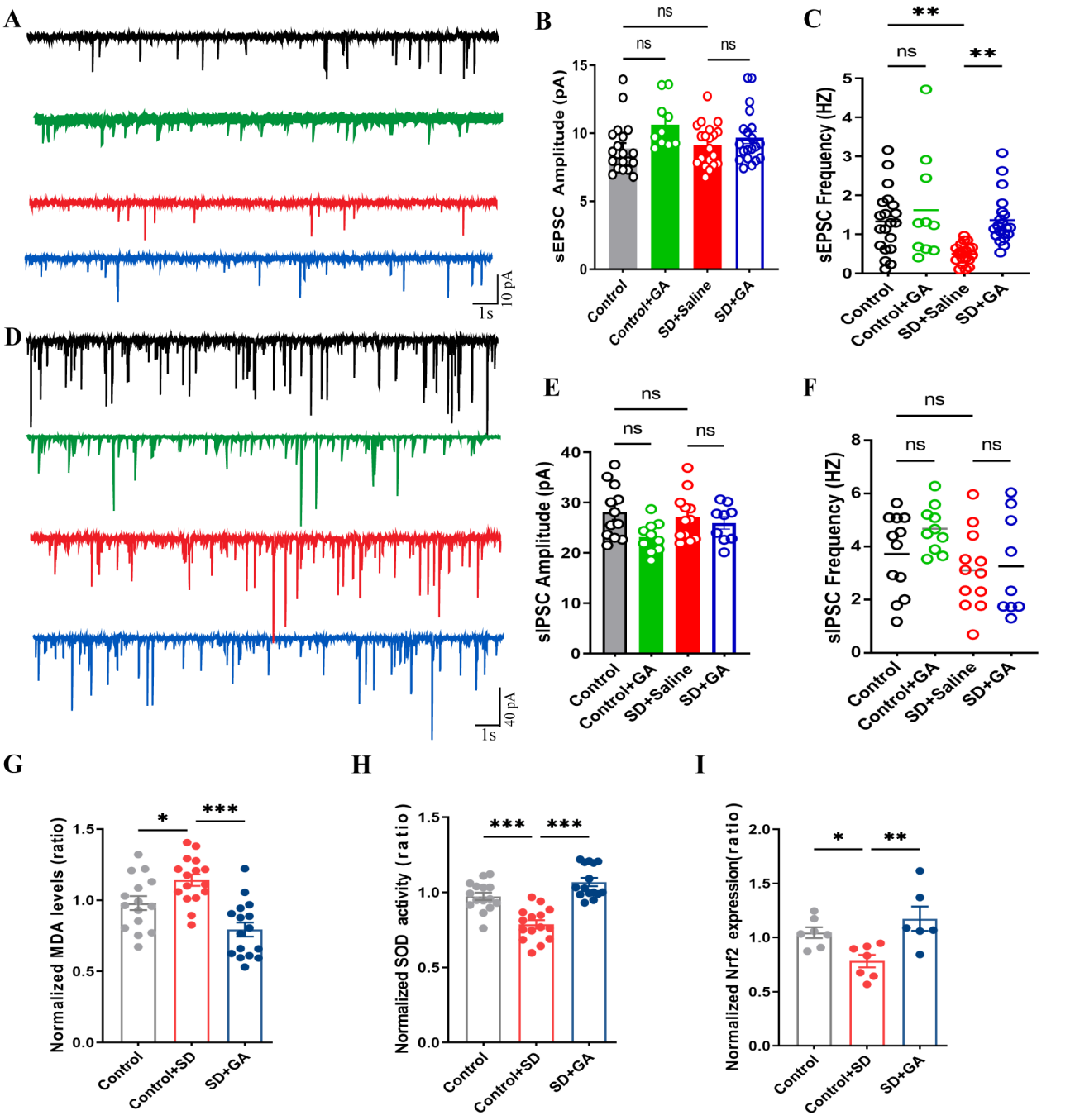

Fig. 6. GA reverse SD-induced synaptic impairment and the change of oxidative stress factor. (A) Sample traces showing sEPSCs. (B) There are no changes of average sEPSC amplitude both in each group. Kolmogorov-Smirnov test, Control vs. SD+Saline, p=0.819; SD+Saline vs. SD+GA, p=0.819. Saline, SD+Saline, SD+GA group, n=20 cells in 5 mice of each group. Control+GA group, n=10 cells in 4 mice. (C)The frequency of sEPSCs is decreased by SD and GA reversed this to control level. One-way ANOVA with Tukey's multiple comparisons test. Control vs. SD+Saline, p =0.05; SD+Saline vs. SD+GA, p =0.04; Control vs. Control+GA, p=0.762. Control, SD+Saline, SD+GA group, n=20 cells in 5 mice of each group. Control+GA group, n=10 cells in 4 mice (D) Sample traces showing sIPSCs. (E, F) The inhibition synaptic transmission in pyramidal neurons is not affected by SD and GA. Amplitude: Kolmogorov-Smirnov test, Control vs. SD+Saline, p=0.847; SD+Saline vs. SD+GA, p=0.99. Frequency: one-way ANOVA with Tukey's test. Control vs. SD+Saline, p=0.739; SD+Saline vs. SD+GA, p=0.996; Control vs. Control+GA, p=0.443. n=12 cells in 4 Control mice, n=12 cells in 4 SD+Saline mice, n=9 cells in 4 SD+GA mice, n=10 cells in 4 Control+GA mice. (G, H) The levels of MDA and the activity of SOD detected by spectrophotometric method. One-way ANOVA with Tukey's test. MDA: Control vs. Control+SD, p=0.047; Control+SD vs. SD+GA, p<0.001. n=16 mice per group. SOD: Control vs. Control+SD, p<0.001; Control+SD vs. SD+GA, p<0.001. n=15 mice per group. (I) The expression of Nrf2 in the cortex detected by Elisa. One-way ANOVA with Tukey's test. Control vs. Control+SD, p=0.049; Control+SD vs. SD+GA, p=0.005. n=a. All data are shown as mean±SEM. ***p<0.001, **p<0.01, *p<0.05, ns, not significant.

40% compared to the initial value [39]. Moreover, sleep loss altered the relative expression levels of the AMPA and NMDA type receptors [40]. As the glutamate receptor subunits play a crucial role in regulating Ca^{2+} entry into cells, they may be essential in determining excitability and synaptic plasticity [1, 41].

In addition to SD may have different effects on different brain regions, the duration of SD has an important impact on cognitive function, the function and morphological structure of neurons, and synaptic plasticity [42]. Our previous research found that the effects SD with different periods (24 h, 48 h, 72 h) on the cognition of mice and the morphological structure and synaptic plasticity of hippocampal neurons were significantly different. 24 h SD improved the object location memory (OLM) of mice, accompanied by a significantly increased hippocampal synaptic plasticity, including gain of dendritic spines, increased expression of hippocampal GluA1, and enhanced long-term potentiation (LTP). 48 h SD showed no effect on OLM or the hippocampal synaptic plasticity mentioned above. However, 72 h SD impaired novelty-related OLM and weakened hippocampal synaptic plasticity, including serious loss of dendritic spines, decreased expression of hippocampal GluA1, and significantly attenuated LTP [43]. In this study, we found that the spatial learning and memory deficits of mice were decreased, the frequency and amplitude of Ca^{2+} transients were reduced while the proportions of inactive neurons in layer 2/3 of ACC was increased, and the frequency of sEPSC in layer 2/3 of ACC was significantly decreased with 72 h SD. These results are similar to those in our previous study for 72 h SD. But different from our previous study, the two-photon imaging results of this study showed that the neural excitability in 2/3 layer of ACC was not increased but decreased with 24 h SD, which may be related to different brain areas, the hippocampus in our previous study and ACC in this study. Our results also found that the administration of GA notably mitigated the decline of calcium transients in ACC neurons. The effects of GA may be related to its antioxidation.

A balance exists between the antioxidant capacity and reactive oxygen species (ROS) within the body. Disruption of this balance results in oxidative stress, leading to irreversible damage to biological macromolecules such as DNA, lipids, and proteins [5]. Both preclinical and clinical studies have established that memory impairments are associated with an oxidant-antioxidant imbalance in numerous situations [43, 44]. Binding of glutamate and postsynaptic depolarization results in NMDAR activation and an influx of Ca^{2+} to induce LTP. The increase in intracellular Ca^{2+} initiates a modest and reversible increase in ROS, and in turn, ROS inhibits NMDAR activity. As oxidative stress increases, ROS has effects on NMDARs that result in a further dysregulation of Ca^{2+} homeostasis. In that way, NMDARs remain hyporesponsive and reduce the influx of Ca^{2+} and activity of CaMKII, contributing to impaired LTP induction and neural excitability [45]. Oxidative damage does not influence AMPA receptor-mediated synaptic transmission. Rather, the decrease in AMPA receptor-mediated synaptic transmission during oxidative stress is ancillary to NMDA receptor hypofunction and impaired synaptic transmission and plasticity [45, 46]. There is no consensus concerning the influence of oxidative stress on GABA release, which may depend on the brain region examined [45, 47].

In line with previous reports [48], our study showed that SD significantly elevated oxidative stress levels by reducing the expression of Nrf2 and antioxidant enzyme SOD activities and increasing MDA content in the PFC. Concurrently, GA administration notably counteracted oxidative stress damage with increased neural excitability and excitatory synaptic transmission from SD, potentially explaining the beneficial effects on cognitive performance in SD-treated mice. Earlier reports demonstrated that Ellagic acid, a dimer of gallic acid [49], improved recognition memory by increasing SOD activity while reducing ROS levels in the hippocampus in SD-induced mice through the Nrf2 pathway [50].

Additionally, Nrf2, which is widely expressed in eukaryotic cells, has been considered a critical activator of its downstream antioxidant enzymes, including SOD, and is regarded as one of the most important cellular mechanisms for protection against oxidative stress [51, 52]. The current study revealed that the expressions of Nrf2 and its downstream targets in the PFC of mice were significantly inhibited after SD, while GA treatment reversed this phenomenon [53]. As such, the detrimental effects of increased oxidative stress on memory functions during SD may be mediated by the suppression of signaling molecules essential for memory processing, such as Nrf2. GA, with its antioxidant properties, could protect cognitive performance by preventing this sequence of events during SD.

In conclusion, this study confirmed that the protective effect of GA on 72 h sleep-deprived mice primarily involves aspects of neuronal activity and excitatory synaptic transmission function. It was demonstrated that GA can alleviate neuronal hyperactivity and abnormal calcium influx by regulating excessive glutamate synaptic transmission induced by SD, potentially through mitigating oxidative stress levels in the central nervous system (CNS). These findings suggest that, GA, a small molecule polyphenol widely found in plants [54], may serve as a potential candidate agent for preventing and treating cognitive impairments induced by sleep deprivation.

https://doi.org/10.5607/en23015

ACKNOWLEDGEMENTS

We thank Dr. Zhijuan Zheng, Dr. Chuanguo Liu and Xuehuan Liu from Experiment Center, Shandong University of Traditional Chinese Medicine for their technical support.

CONFLICT OF INTEREST

The authors declare that they have no competing interests.

REFERENCES

1. Havekes R, Abel T (2017) The tired hippocampus: the molecular impact of sleep deprivation on hippocampal function. Curr Opin Neurobiol 44:13-19.
2. Li W, Ma L, Yang G, Gan WB (2017) REM sleep selectively prunes and maintains new synapses in development and learning. Nat Neurosci 20:427-437.
3. Noble W, Spires-Jones TL (2019) Sleep well to slow Alzheimer's progression? Science 363:813-814.
4. Hossain MF, Wang N, Chen R, Li S, Roy J, Uddin MG, Li Z, Lim LW, Song YQ (2021) Exploring the multifunctional role of melatonin in regulating autophagy and sleep to mitigate Alzheimer's disease neuropathology. Ageing Res Rev 67:101304.
5. Lu C, Lv J, Jiang N, Wang H, Huang H, Zhang L, Li S, Zhang N, Fan B, Liu X, Wang F (2020) Protective effects of genistein on the cognitive deficits induced by chronic sleep deprivation. Phytother Res 34:846-858.
6. Montes-Rodríguez CJ, Rueda-Orozco PE, Prospéro-García O (2019) Total sleep deprivation impairs fear memory retrieval by decreasing the basolateral amygdala activity. Brain Res 1719:17-23.
7. Alzoubi KH, Al Mosabih HS, Mahasneh AF (2019) The protective effect of edaravone on memory impairment induced by chronic sleep deprivation. Psychiatry Res 281:112577.
8. Krause AJ, Simon EB, Mander BA, Greer SM, Saletin JM, Goldstein-Piekarski AN, Walker MP (2017) The sleep-deprived human brain. Nat Rev Neurosci 18:404-418.
9. Ma N, Dinges DF, Basner M, Rao H (2015) How acute total sleep loss affects the attending brain: a meta-analysis of neuroimaging studies. Sleep 38:233-240.
10. Leinweber M, Ward DR, Sobczak JM, Attinger A, Keller GB (2017) A sensorimotor circuit in mouse cortex for visual flow predictions. Neuron 96:1204.
11. Koike H, Demars MP, Short JA, Nabel EM, Akbarian S, Baxter MG, Morishita H (2016) Chemogenetic inactivation of dorsal anterior cingulate cortex neurons disrupts attentional behavior in mouse. Neuropsychopharmacology 41:1014-1023.
12. Zhang S, Xu M, Kamigaki T, Hoang Do JP, Chang WC, Jenvay S, Miyamichi K, Luo L, Dan Y (2014) Selective attention. Long-range and local circuits for top-down modulation of visual cortex processing. Science 345:660-665.
13. Vaccaro A, Kaplan Dor Y, Nambara K, Pollina EA, Lin C, Greenberg ME, Rogulja D (2020) Sleep loss can cause death through accumulation of reactive oxygen species in the gut. Cell 181:1307-1328.e15.
14. Sabia S, Fayosse A, Dumurgier J, van Hees VT, Paquet C, Sommerlad A, Kivimäki M, Dugravot A, Singh-Manoux A (2021) Association of sleep duration in middle and old age with incidence of dementia. Nat Commun 12:2289.
15. Trivedi MS, Holger D, Bui AT, Craddock TJA, Tartar JL (2017) Short-term sleep deprivation leads to decreased systemic redox metabolites and altered epigenetic status. PLoS One 12:e0181978.
16. Buzsáki G, Wang XJ (2012) Mechanisms of gamma oscillations. Annu Rev Neurosci 35:203-225.
17. Samad N, Jabeen S, Imran I, Zulfiqar I, Bilal K (2019) Protective effect of gallic acid against arsenic-induced anxiety-/depression- like behaviors and memory impairment in male rats. Metab Brain Dis 34:1091-1102.
18. Mirshekari Jahangiri H, Sarkaki A, Farbood Y, Dianat M, Goudarzi G (2020) Gallic acid affects blood-brain barrier permeability, behaviors, hippocampus local EEG, and brain oxidative stress in ischemic rats exposed to dusty particulate matter. Environ Sci Pollut Res Int 27:5281-5292.
19. Badhani B, Kakkar R (2017) In silico studies on potential MCF-7 inhibitors: a combination of pharmacophore and 3D-QSAR modeling, virtual screening, molecular docking, and pharmacokinetic analysis. J Biomol Struct Dyn 35:1950-1967.
20. Liu YL, Hsu CC, Huang HJ, Chang CJ, Sun SH, Lin AM (2020) Gallic acid attenuated LPS-induced neuroinflammation: protein aggregation and necroptosis. Mol Neurobiol 57:96-104.
21. Bowers SJ, Lambert S, He S, Lowry CA, Fleshner M, Wright KP, Turek FW, Vitaterna MH (2021) Immunization with a heat-killed bacterium, mycobacterium vaccae NCTC 11659, prevents the development of cortical hyperarousal and a PTSD-like sleep phenotype after sleep disruption and acute stress in mice. Sleep 44:zsaa271.
22. Tabassum S, Misrani A, Tabassum S, Ahmed A, Yang L, Long C (2021) Disrupted prefrontal neuronal oscillations and morphology induced by sleep deprivation in young APP/PS1 transgenic AD mice. Brain Res Bull 166:12-20.
23. Yang SQ, Jiang L, Lan F, Wei HJ, Xie M, Zou W, Zhang P, Wang

CY, Xie YR, Tang XQ (2019) Inhibited endogenous H2S generation and excessive autophagy in hippocampus contribute to sleep deprivation-induced cognitive impairment. Front Psychol 10:53.

24. Kraeuter AK, Guest PC, Sarnyai Z (2019) The Y-maze for assessment of spatial working and reference memory in mice. Methods Mol Biol 1916:105-111.
25. Huda R, Sipe GO, Breton-Provencher V, Cruz KG, Pho GN, Adam E, Gunter LM, Sullins A, Wickersham IR, Sur M (2020) Distinct prefrontal top-down circuits differentially modulate sensorimotor behavior. Nat Commun 11:6007.
26. Hattori R, Komiyama T (2022) Longitudinal two-photon calcium imaging with ultra-large cranial window for head-fixed mice. STAR Protoc 3:101343.
27. Li J, Tian C, Yuan S, Yin Z, Wei L, Chen F, Dong X, Liu A, Wang Z, Wu T, Tian C, Niu L, Wang L, Wang P, Xie W, Cao F, Shen H (2023) Neuropathic pain following spinal cord hemisection induced by the reorganization in primary somatosensory cortex and regulated by neuronal activity of lateral parabrachial nucleus. CNS Neurosci Ther. doi: 10.1111/cns.14258.
28. Patel TP, Man K, Firestein BL, Meaney DF (2015) Automated quantification of neuronal networks and single-cell calcium dynamics using calcium imaging. J Neurosci Methods 243:26-38.
29. Mishra R, Manchanda S, Gupta M, Kaur T, Saini V, Sharma A, Kaur G (2016) Tinospora cordifolia ameliorates anxiety-like behavior and improves cognitive functions in acute sleep deprived rats. Sci Rep 6:25564.
30. Frau R, Traccis F, Bortolato M (2020) Neurobehavioural complications of sleep deprivation: shedding light on the emerging role of neuroactive steroids. J Neuroendocrinol 32:e12792.
31. Misrani A, Tabassum S, Wang M, Chen J, Yang L, Long C (2020) Citalopram prevents sleep-deprivation-induced reduction in CaMKII-CREB-BDNF signaling in mouse prefrontal cortex. Brain Res Bull 155:11-18.
32. McDermott CM, Hardy MN, Bazan NG, Magee JC (2006) Sleep deprivation-induced alterations in excitatory synaptic transmission in the CA1 region of the rat hippocampus. J Physiol 570(Pt 3):553-565.
33. Yang RH, Wang WT, Hou XH, Hu SJ, Chen JY (2010) Ionic mechanisms of the effects of sleep deprivation on excitability in hippocampal pyramidal neurons. Brain Res 1343:135-142.
34. Tartar JL, McKenna JT, Ward CP, McCarley RW, Strecker RE, Brown RE (2010) Sleep fragmentation reduces hippocampal CA1 pyramidal cell excitability and response to adenosine. Neurosci Lett 469:1-5.
35. Zhang K, Lian N, Ding R, Guo C, Dong X, Li Y, Wei S, Jiao Q, Yu Y, Shen H (2020) Sleep deprivation aggravates cognitive impairment by the alteration of hippocampal neuronal activity and the density of dendritic spine in isoflurane-exposed mice. Front Behav Neurosci 14:589176.
36. Winters BD, Huang YH, Dong Y, Krueger JM (2011) Sleep loss alters synaptic and intrinsic neuronal properties in mouse prefrontal cortex. Brain Res 1420:1-7.
37. Liu ZW, Faraguna U, Cirelli C, Tononi G, Gao XB (2010) Direct evidence for wake-related increases and sleep-related decreases in synaptic strength in rodent cortex. J Neurosci 30:8671-8675.
38. Crick F, Mitchison G (1983) The function of dream sleep. Nature 304:111-114.
39. Dash MB, Douglas CL, Vyazovskiy VV, Cirelli C, Tononi G (2009) Long-term homeostasis of extracellular glutamate in the rat cerebral cortex across sleep and waking states. J Neurosci 29:620-629.
40. Xie M, Yan J, He C, Yang L, Tan G, Li C, Hu Z, Wang J (2015) Short-term sleep deprivation impairs spatial working memory and modulates expression levels of ionotropic glutamate receptor subunits in hippocampus. Behav Brain Res 286:64-70.
41. Kreutzmann JC, Havekes R, Abel T, Meerlo P (2015) Sleep deprivation and hippocampal vulnerability: changes in neuronal plasticity, neurogenesis and cognitive function. Neuroscience 309:173-190.
42. Jiao Q, Dong X, Guo C, Wu T, Chen F, Zhang K, Ma Z, Sun Y, Cao H, Tian C, Hu Q, Liu N, Wang Y, Ji L, Yang S, Zhang X, Li J, Shen H (2022) Effects of sleep deprivation of various durations on novelty-related object recognition memory and object location memory in mice. Behav Brain Res 418:113621.
43. Singh A, Kukreti R, Saso L, Kukreti S (2019) Oxidative stress: a key modulator in neurodegenerative diseases. Molecules 24:1583.
44. Liguori I, Russo G, Curcio F, Bulli G, Aran L, Della-Morte D, Gargiulo G, Testa G, Cacciatore F, Bonaduce D, Abete P (2018) Oxidative stress, aging, and diseases. Clin Interv Aging 13:757-772.
45. Kumar A, Yegla B, Foster TC (2018) Redox signaling in neurotransmission and cognition during aging. Antioxid Redox Signal 28:1724-1745.
46. Lu C, Chan SL, Haughey N, Lee WT, Mattson MP (2001) Selective and biphasic effect of the membrane lipid peroxidation product 4-hydroxy-2,3-nonenal on N-methyl-D-aspartate channels. J Neurochem 78:577-589.
47. Bradley SA, Steinert JR (2016) Nitric oxide-mediated post-

translational modifications: impacts at the synapse. Oxid Med Cell Longev 2016:5681036.
48. Nabaee E, Kesmati M, Shahriari A, Khajehpour L, Torabi M (2018) Cognitive and hippocampus biochemical changes following sleep deprivation in the adult male rat. Biomed Pharmacother 104:69-76.
49. Javaid N, Shah MA, Rasul A, Chauhdary Z, Saleem U, Khan H, Ahmed N, Uddin MS, Mathew B, Behl T, Blundell R (2021) Neuroprotective effects of ellagic acid in Alzheimer's disease: focus on underlying molecular mechanisms of therapeutic potential. Curr Pharm Des 27:3591-3601.
50. Wang W, Yang L, Liu T, Wang J, Wen A, Ding Y (2020) Ellagic acid protects mice against sleep deprivation-induced memory impairment and anxiety by inhibiting TLR4 and activating Nrf2. Aging (Albany NY) 12:10457-10472.
51. Jiao W, Wang Y, Kong L, Ou-Yang T, Meng Q, Fu Q, Hu Z (2018) CART peptide activates the Nrf2/HO-1 antioxidant pathway and protects hippocampal neurons in a rat model of Alzheimer's disease. Biochem Biophys Res Commun 501:1016-1022.
52. Lu J, Wang Z, Cao J, Chen Y, Dong Y (2018) A novel and compact review on the role of oxidative stress in female reproduction. Reprod Biol Endocrinol 16:80.
53. Pandurangan AK, Mohebali N, Norhaizan ME, Looi CY (2015) Gallic acid attenuates dextran sulfate sodium-induced experimental colitis in BALB/c mice. Drug Des Devel Ther 9:3923-3934.
54. Al Zahrani NA, El-Shishtawy RM, Asiri AM (2020) Recent developments of gallic acid derivatives and their hybrids in medicinal chemistry: a review. Eur J Med Chem 204:112609.